



Article

Resveratrol Protects against Zearalenone-Induced Mitochondrial Defects during Porcine Oocyte Maturation via PINK1/Parkin-Mediated Mitophagy

Jiehuan Xu ^{1,2,3}, Lingwei Sun ^{1,2} , Mengqian He ^{1,2}, Shushan Zhang ^{1,2,3,4}, Jun Gao ^{1,4} , Caifeng Wu ^{1,4}, Defu Zhang ^{1,2,3,4,*} and Jianjun Dai ^{1,2,3,4,*}

¹ Institute of Animal Husbandry and Veterinary Science, Shanghai Academy of Agricultural Sciences, Shanghai 201106, China

² Shanghai Municipal Key Laboratory of Agri-Genetics and Breeding, Shanghai 201106, China

³ Shanghai Engineering Research Center of Breeding Pig, Shanghai 201106, China

⁴ Key Laboratory of Livestock and Poultry Resources (Pig) Evaluation and Utilization, Ministry of Agriculture and Rural Affairs, Shanghai 201106, China

* Correspondence: zhangdefu@saas.sh.cn (D.Z.); daijianjun@saas.sh.cn (J.D.)

Abstract: Mitochondria hold redox homeostasis and energy metabolism as a crucial factor during oocyte maturation, while the exposure of estrogenic mycotoxin zearalenone causes developmental incapacity in porcine oocyte. This study aimed to reveal a potential resistance of phytoalexin resveratrol against zearalenone during porcine oocyte maturation and whether its mechanism was related with PTEN-induced kinase 1 (PINK1)/Parkin-mediated mitophagy. Porcine oocytes were exposed to 20 μ M zearalenone with or without 2 μ M resveratrol during in vitro maturation. As for the results, zearalenone impaired ultrastructure of mitochondria, causing mitochondrial depolarization, oxidative stress, apoptosis and embryonic developmental incapacity, in which mitophagy was induced in response to mitochondrial dysfunction. Phytoalexin resveratrol enhanced mitophagy through PINK1/Parkin in zearalenone-exposed oocytes, manifesting as enhanced mitophagy flux, upregulated PINK1, Parkin, microtubule-associated protein light-chain 3 beta-II (LC3B-II) and down-regulated substrates mitofusin 2 (MFN2), voltage-dependent anion channels 1 (VDAC1) and p62 expressions. Resveratrol redressed zearalenone-induced mitochondrial depolarization, oxidative stress and apoptosis, and accelerated mitochondrial DNA copy during maturation, which improved embryonic development. This study offered an antitoxin solution during porcine oocyte maturation and revealed the involvement of PINK1/Parkin-mediated mitophagy, in which resveratrol mitigated zearalenone-induced embryonic developmental incapacity.

Keywords: zearalenone; mitophagy; resveratrol; PINK1/Parkin; porcine oocyte

Key Contribution: The application of phytoalexin resveratrol redresses oocyte developmental incapacity against zearalenone contamination. PINK1/Parkin-mediated mitophagy is involved in the antitoxin effect of resveratrol.



Citation: Xu, J.; Sun, L.; He, M.; Zhang, S.; Gao, J.; Wu, C.; Zhang, D.; Dai, J. Resveratrol Protects against Zearalenone-Induced Mitochondrial Defects during Porcine Oocyte Maturation via PINK1/Parkin-Mediated Mitophagy. *Toxins* **2022**, *14*, 641. <https://doi.org/10.3390/toxins14090641>

Received: 9 August 2022

Accepted: 14 September 2022

Published: 16 September 2022

Publisher's Note: MDPI stays neutral with regard to jurisdictional claims in published maps and institutional affiliations.



Copyright: © 2022 by the authors. Licensee MDPI, Basel, Switzerland. This article is an open access article distributed under the terms and conditions of the Creative Commons Attribution (CC BY) license (<https://creativecommons.org/licenses/by/4.0/>).

1. Introduction

Grains are major ingredients in feed formulation in intensive livestock farms, while around 70% of cereal feeds is polluted by mycotoxins [1]. Zearalenone is a non-steroidal estrogenic mycotoxin produced by multiple species of the *Fusarium* genus that is frequently detected in cereals [2]. Based on a ten-year global survey from more than 74,000 samples in 100 countries, zearalenone is one of the top-three mycotoxins in animal feedstuffs [3]. Serious studies have reported that zearalenone and its metabolites have estrogen-like activities in human and domestic animals that compete with the estrogen receptor [4]. As a result, excessive estrogen syndrome and a series of pathological changes in the reproductive

organs occur in domestic animals through ingestion of zearalenone-polluted fodder [5], causing economic loss to husbandry and the culling of breeding stocks.

As a main livestock and medical model, pigs have been considered more sensitive to zearalenone toxicity [6]. High-dose zearalenone intake causes permanent pathologic alterations in pigs, leading to edema and prolapse of the vagina, infertility, pseudopregnancy and embryo lethal resorption [7]. The toxicity of zearalenone on porcine oocytes is presumed to relate to oxidative stress, apoptosis, autophagy and epigenetic modification variation [8]. Similar research on porcine blastocysts also claimed that zearalenone exposure promoted DNA damage, apoptosis and autophagy [9]. Other studies demonstrated that zearalenone exposure impaired mitochondrial membrane potential ($\Delta\Psi_m$) [10], causing oxidative stress through the mitochondrial apoptosis pathway in pigs [11]. These studies hinted the state of mitochondria as a presumable toxicology of zearalenone, while in this study, further disclosure of their interrelation and potential rescue solution of in vitro maturation (IVM) oocytes will be evaluated.

Each oocyte equips a large supply of mitochondria to meet the energy requirement of maturation and embryonic development. Mitochondria are a crucial factor determining the developmental competence of oocytes, as they control intracellular Ca^{2+} homeostasis and produce ATP for continuous transcription and translation [12]. During mitochondrial renewal or mitochondrial stress, mitophagy, oocytes selectively degrading impaired or supernumerary mitochondria through autophagy, are involved in maintaining mitochondrial homeostasis and oocyte survival [13].

As an evolutionarily conserved intracellular function, autophagy is considered a stress-responsive autonomous process. Cells selectively dispose of redundant, potentially harmful or dysfunctional cytoplasmic entities via autophagy to maintain intracellular homeostasis [14]. Mitophagy, selectively eliminating mitochondria via autophagy, is critical for the quality and quantity control of mitochondria. Impaired mitochondria are targeted by the autophagic system to form mitophagosomes and subsequently delivered to lysosomes for degradation. A primary signaling pathway to regulate mitophagy is through ubiquitin-dependent PTEN-induced kinase 1 (PINK1)/Parkin. PINK1, a Ser/Thr kinase, stabilizes on depolarized mitochondria and phosphorylates mitofusin (MFN), voltage-dependent anion channels 1 (VDAC1) and other substrates on the outer-mitochondrial membrane (OMM) [15,16]. E3 ubiquitin ligase Parkin is then recruited by phosphorylated substrates from cytoplasm to depolarized mitochondria and catalyzes the transferring of ubiquitin to substrates on OMM [17,18]. These polyubiquitinated substrates are recognized by p62 and interact with microtubule-associated protein light chain 3 (LC3) through LC3-interacting region motif and further cause the bilayer membrane structure to encapsulate damaged mitochondria. The mitophagosome is then formed. In order to degrade target mitochondria as its cargo inside, fashioned mitophagosome subsequently fused with lysosome, forming mitophagolysosome. Target mitochondria are degraded into matrix substances in the acidic environment of lysosomes and recycled by cell.

Due to cytoplasmic immaturity, the developmental capacity of IVM oocytes is considered lower than ovulatory oocytes [19]. Therefore, numerous antioxidants have been evaluated to rescue IVM oocytes. Resveratrol, a natural phytoalexin, has been widely studied for its resistant properties against oxidation, carcinogenicity and inflammation. A previous study demonstrated multiple effects of resveratrol towards oocytes, such as enhancing the clearance of mitochondrial damage [20], protecting oocytes from oxidative stress and apoptosis, promoting oocyte maturation and hindering postovulatory aging [21]. Recent studies revealed that these beneficial effects are closely related to autophagy/mitophagy induced by resveratrol through multiple signaling pathways. For example, mitophagy and enhanced mitochondrial protein FOXO3a induced by resveratrol was considered as a potential mechanism against postovulatory oocyte aging [22]. In consideration of the antitoxin effect of resveratrol and its close relation with mitophagy, this study presumed a hypothesis that resveratrol could rescue zearalenone-induced maturation impairment of porcine oocyte through PINK1/Parkin-mediated mitophagy. Resveratrol was concurrently

co-incubated with zearalenone during porcine oocyte maturation for the hypothetical resistance against zearalenone.

The purpose of this study was to (1) elucidate whether resveratrol could alleviate zearalenone-induced oxidative stress, apoptosis and developmental incapacity during porcine oocyte maturation through mitophagy and (2) clarify whether the PINK1/Parkin signaling pathway was involved in it.

2. Results

2.1. Resveratrol Alleviated Zearalenone-Induced Embryonic Developmental Failures

To clarify the effect of estrogen-like mycotoxin zearalenone and the hypothetical antitoxin effects of resveratrol against zearalenone during porcine oocyte maturation, parthenogenetic activation (PA) and in vitro zygote culture were performed to determine the cleavage and blastosphere rates as embryonic developmental potential (Figure 1A–C). The results revealed that zearalenone hindered the development of PA embryo, demonstrated as significantly decreased cleavage rate ($90.67\% \pm 3.24\%$ vs. $67.74\% \pm 3.96\%$, $p < 0.05$) and blastosphere rate ($18.64\% \pm 1.98\%$ vs. $7.28\% \pm 1.50\%$, $p < 0.05$). Compared to zearalenone-exposed oocytes, the cleavage rate ($67.74\% \pm 3.96\%$ vs. $82.78\% \pm 2.31\%$, $p < 0.05$) and blastosphere rate ($7.28\% \pm 1.50\%$ vs. $13.20\% \pm 2.23\%$) raised up when resveratrol co-incubated with zearalenone during oocyte maturation.

2.2. Resveratrol Alleviated Zearalenone-Induced Oxidative Stress and Apoptosis during Oocyte Maturation

To reveal the mechanism of embryonic developmental failures induced by zearalenone and the antitoxin effect of resveratrol, oocyte ROS levels (Figure 1D,E) and apoptosis rates (Figure 1F,G) were, respectively, determined. Compared to matured oocytes, zearalenone significantly upregulated the ROS generation (1.00 ± 0.08 vs. 9.23 ± 0.67 , $p < 0.05$) and apoptosis rate ($6.67\% \pm 1.93\%$ vs. $66.02\% \pm 3.31\%$, $p < 0.05$) in porcine oocytes, while, compared to zearalenone-exposed oocytes, resveratrol significantly inhibited the ROS generation (9.23 ± 0.67 vs. 5.89 ± 0.60 , $p < 0.05$) and apoptosis ($66.02\% \pm 3.31\%$ vs. $51.25\% \pm 3.08\%$, $p < 0.05$) when it co-incubated with zearalenone during oocyte maturation.

2.3. Resveratrol Alleviated Zearalenone-Induced Mitochondrial Defects during Oocyte Maturation

To explore the effect of zearalenone towards oocyte mitochondrial state, ultrastructure observation and determinations of $\Delta\Psi_m$ and mitochondrial DNA (mtDNA) copy numbers were performed. As for the results, numerous mitochondria in regular morphology with mitochondrial crista were equably distributed in the cytoplasm in matured porcine oocytes. After zearalenone exposure, the destruction of mitochondrial internal structure, including vacuolated mitochondria and vague or disabled cristae (white arrows), was observed in oocytes. Typical structure of mitophagosome (red arrow) was observed in zearalenone-exposed oocytes (Figure 2A), which indicated the activation of mitophagy.

In the meantime, the ultrastructural damage caused by zearalenone led to the variation in $\Delta\Psi_m$ (Figure 2B,C) and relative mtDNA copy number (Figure 2D), which were determined by fluorescence probe JC-1 and realtime-PCR. As for the results, compared to matured oocytes, the $\Delta\Psi_m$ (1.56 ± 0.08 vs. 0.66 ± 0.08 , $p < 0.05$) and relative mtDNA copy number (1.00 ± 0.11 vs. 0.76 ± 0.08) were both decreased in zearalenone-exposed oocytes. The results above revealed that zearalenone exposure led to mitochondrial structural damage, depolarization and decreased mtDNA copy number and also hinted the involvement of mitophagy in zearalenone-induced mitochondrial defects during porcine oocyte maturation.

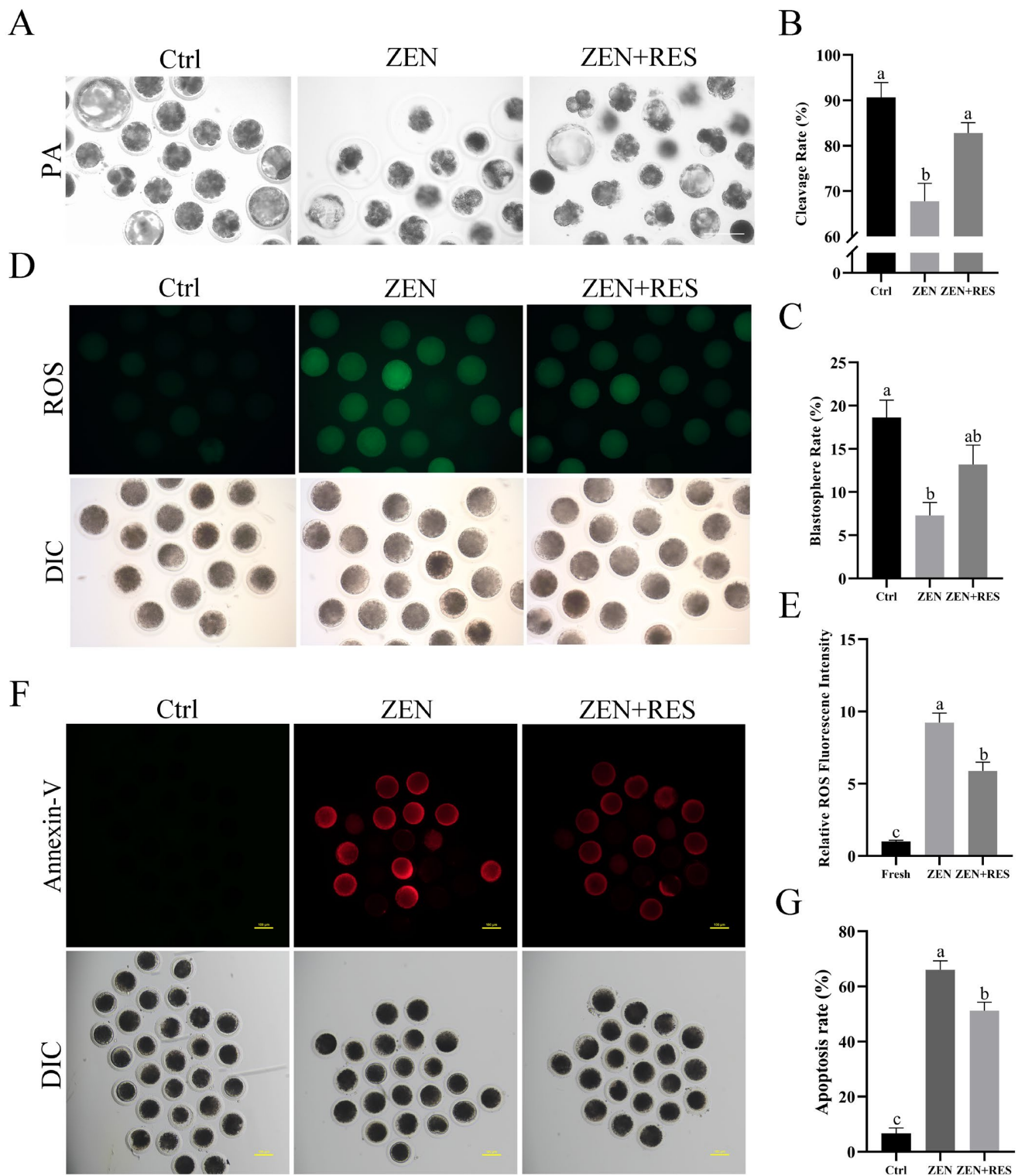


Figure 1. Resveratrol alleviated zearalenone-induced oocyte oxidative stress, early apoptosis and loss of embryonic developmental potential. (A) Morphological observation of PA embryos in 7 d. Bar = 100 μ m. (B,C) Statistical analysis on the ratio of cleavage and blastosphere number. (D) Determination of ROS generation. Bar = 100 μ m. (E) Statistical analysis of ROS generation. (F) Fluorescence observation of oocyte apoptosis. Bar = 100 μ m. (G) Statistical analysis of apoptosis rates. Typical images of each different treatment towards oocytes were present. Independent replications were performed three times in each experiment. Different lowercase letters on the statistical graphs indicated significant differences between treatments (p -value < 0.05).

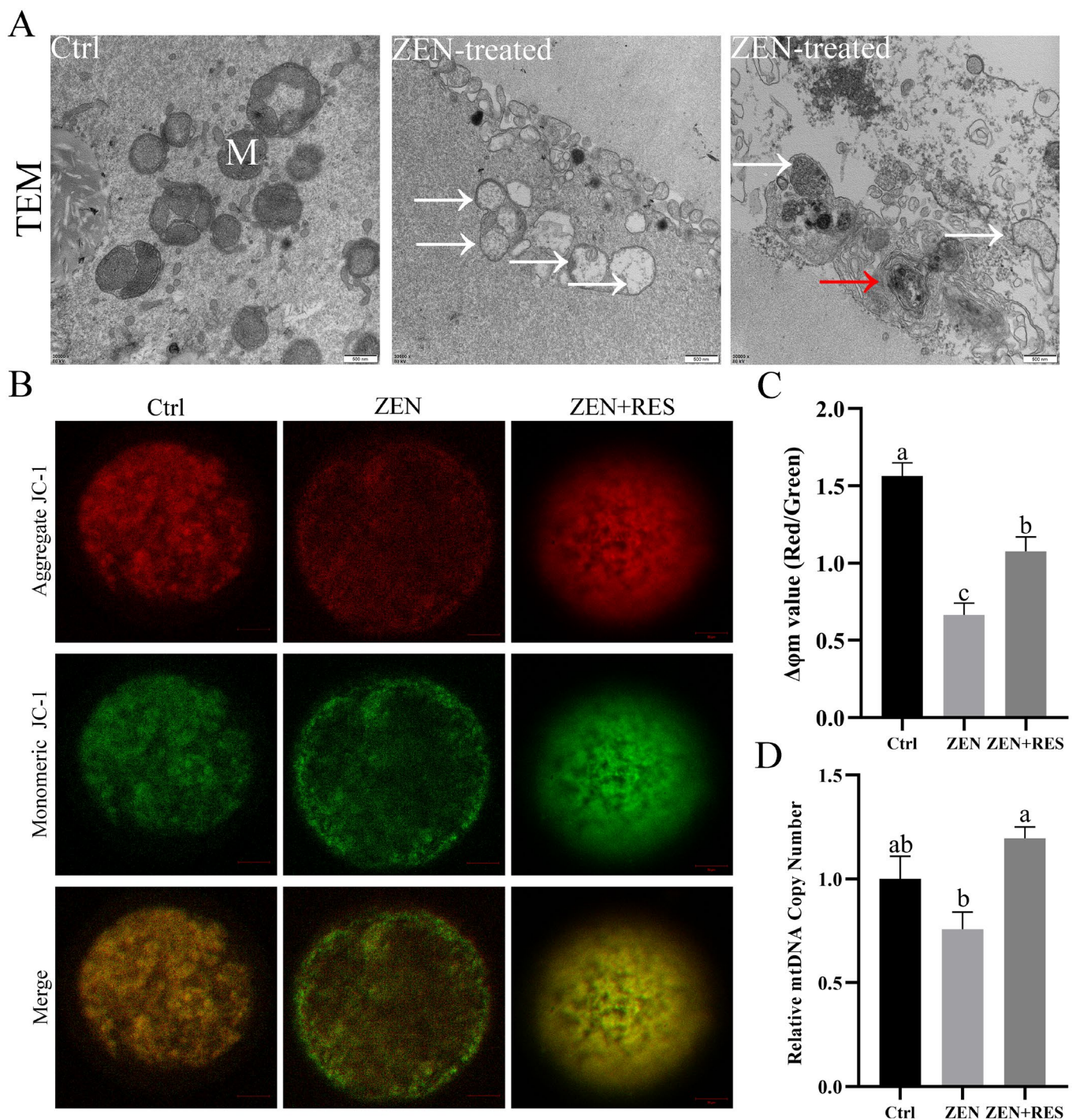


Figure 2. Resveratrol alleviated zearalenone-induced mitochondrial dysfunction during porcine oocyte maturation. (A) Mitochondrial ultrastructure of zearalenone-exposed porcine oocytes was observed by transmission electron microscopy. M: mitochondria. White arrows: damaged mitochondria with vague or disabled cristae. Red arrow: mitophagosome. Bar = 500 nm. (B) Detection of $\Delta\Psi_m$. Red fluorescence represented high $\Delta\Psi_m$ while green fluorescence represented low $\Delta\Psi_m$. Bar = 20 μm . (C) Statistical analysis of $\Delta\Psi_m$ value (Red/Green). (D) Comparison on relative mtDNA copy numbers. Relative gene expression of NADH dehydrogenase subunit 1 (ND1) was determined by real-time PCR. Typical ultrastructural images or intracellular fluorescence images were given representing different oocyte treatments. Independent replications were performed three times in each treatment. Different lowercase letters on the statistical graphs indicated significant differences between treatments (p -value < 0.05).

To explore the effect of resveratrol on mitochondrial defects against zearalenone, $\Delta\Psi_m$ and relative mtDNA copy numbers were determined when resveratrol was co-incubating with zearalenone during porcine oocyte maturation (Figure 2B–D). As for the results, resveratrol significantly upregulated the $\Delta\Psi_m$ (0.66 ± 0.08 vs. 1.08 ± 0.09 , $p < 0.05$) and relative mtDNA copy number (0.76 ± 0.08 vs. 1.20 ± 0.05 , $p < 0.05$) in zearalenone-exposed oocytes. The results revealed that resveratrol alleviated zearalenone-induced mitochondrial defects in porcine oocytes during maturation.

2.4. Resveratrol Enhanced Mitophagy Flux during the Maturation of Zearalenone-Exposed Oocytes

To reveal the mechanism of resveratrol alleviating zearalenone-induced mitochondrial dysfunction and the effect of resveratrol on mitophagy flux in zearalenone-exposed oocytes, the formation and degradation of mitophagosomes were, respectively, determined. Representing the formation of mitophagosomes, mitochondrial outer-membrane marker translocase of outer-mitochondrial membrane 20 (TOMM20) and autophagic vacuole marker microtubule-associated protein 1 light-chain 3 beta (LC3B) were stained using immunofluorescence and colocalized under a laser scanning confocal microscope (LSCM) (Carl Zeiss, Jena, Germany) (Figure 3). After oocyte exposing to zearalenone during maturation, the fraction of TOMM20 overlapping LC3B significantly raised up (0.30 ± 0.04 vs. 0.63 ± 0.06 , $p < 0.05$). Compared to it, resveratrol further upregulated the formation of mitophagosomes in zearalenone-exposed oocytes, demonstrating a significantly enhanced fraction of TOMM20 overlapping LC3B (0.63 ± 0.06 vs. 0.88 ± 0.05 , $p < 0.05$).

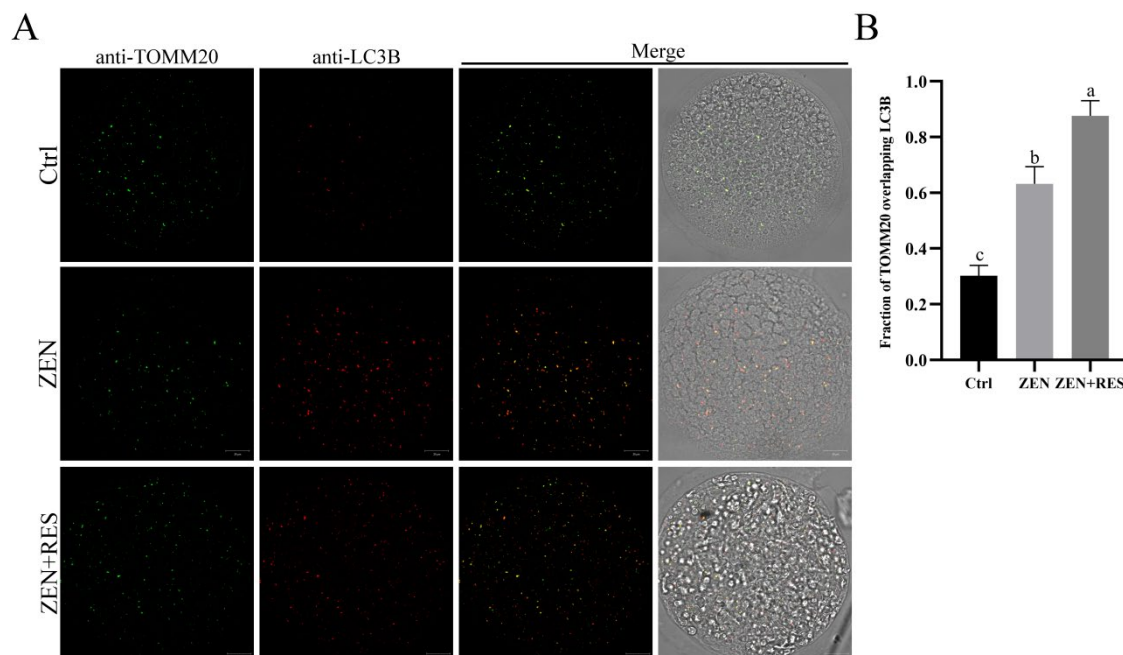


Figure 3. Fluorescence colocalization of mitophagosomes in porcine oocytes. (A) Fluorescence colocalization between VDAC1 and LC3B. Bar = 20 μm . (B) Statistical analysis of the fraction of VDAC1 overlapping LC3B. Typical images of each different treatment towards oocytes were present. Independent replications were performed three times. Different lowercase letters on the statistical graphs indicated significant differences between treatments (p -value < 0.05).

Representing the formation of mitophagolysosomes, the fluorescence colocalization of mitochondria and lysosomes was stained by fluorescence probes Mito-tracker green and Lyso-tracker red and observed under LSCM (Figure 4). The fluorescence dots of mitochondria and lysosomes equally distributed in matured oocytes, showing a loose bond between mitochondria and lysosomes. Compared to it, the colocalization coefficient between mitochondria and lysosomes significantly upregulated in zearalenone-exposed oocytes (0.13 ± 0.02 vs. 0.33 ± 0.04 , $p < 0.05$), which revealed the enhanced formation of

mitophagolysosomes induced by zearalenone. Compared to zearalenone-exposed oocytes, the colocalization coefficient was further upregulated (0.33 ± 0.04 vs. 0.54 ± 0.06 , $p < 0.05$) when resveratrol co-incubated with zearalenone during oocyte maturation.

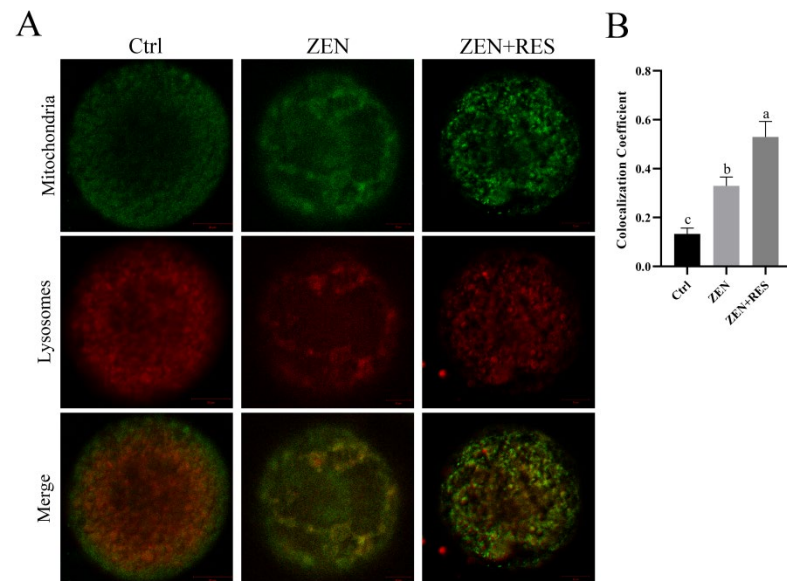


Figure 4. Fluorescence colocalization of mitophagolysosomes in porcine oocytes. **(A)** The fluorescence of mitochondria (represented in green) and lysosomes (represented in red) was inspected by LSCM. Bar = 20 μ m. Typical images of each different treatment towards oocytes were present. Independent replications were performed three times. **(B)** Statistical analysis of colocalization coefficient. Different lowercase letters on the statistical graphs indicated significant differences between treatments (p -value < 0.05).

The results above revealed that mitophagy was activated in zearalenone-exposed porcine oocytes. Based on it, antioxidant resveratrol further enhanced mitophagy flux in zearalenone-exposed oocytes.

2.5. Resveratrol Enhanced Mitophagy through PINK1/Parkin Signaling Pathway in Zearalenone-Exposed Oocytes

To reveal the mechanism of resveratrol altering mitophagy flux in zearalenone-exposed oocytes, the fluorescence aggregation of Parkin and the protein expressions of PINK1/Parkin, a primary signaling pathway of mitophagy, were determined by immunofluorescence and Western blotting. The results showed that, compared to zearalenone-exposed oocytes, resveratrol significantly enhanced fluorescence aggregation of Parkin during oocyte maturation (1.56 ± 0.16 vs. 2.31 ± 0.14 , $p < 0.05$) (Figure 5A,B).

Meanwhile, the results of the Western blot assay revealed that mitophagy was induced by zearalenone in porcine oocyte during maturation (Figure 5B,C), demonstrated as significantly upregulated autophagy marker LC3B-II (0.44 ± 0.03 vs. 0.56 ± 0.03 , $p < 0.05$), and p62 degradation (1.06 ± 0.06 vs. 0.72 ± 0.04 , $p < 0.05$), comparing zearalenone-exposed oocytes to matured oocytes. Meanwhile, compared to zearalenone-exposed oocytes, resveratrol upregulated the protein expressions of the PINK1/Parkin signaling pathway, demonstrated as significantly upregulated PINK1 (0.48 ± 0.04 vs. 0.64 ± 0.03 , $p < 0.05$), Parkin (1.01 ± 0.04 vs. 1.34 ± 0.06 , $p < 0.05$), significant degradation of ubiquitinated substrates VDAC1 (0.73 ± 0.03 vs. 0.49 ± 0.02 , $p < 0.05$) and MFN2 (1.02 ± 0.04 vs. 0.36 ± 0.05 , $p < 0.05$) and significantly upregulated downstream autophagy marker LC3B-II (0.56 ± 0.03 vs. 0.77 ± 0.04 , $p < 0.05$) and p62 degradation (0.73 ± 0.04 vs. 0.40 ± 0.05 , $p < 0.05$).

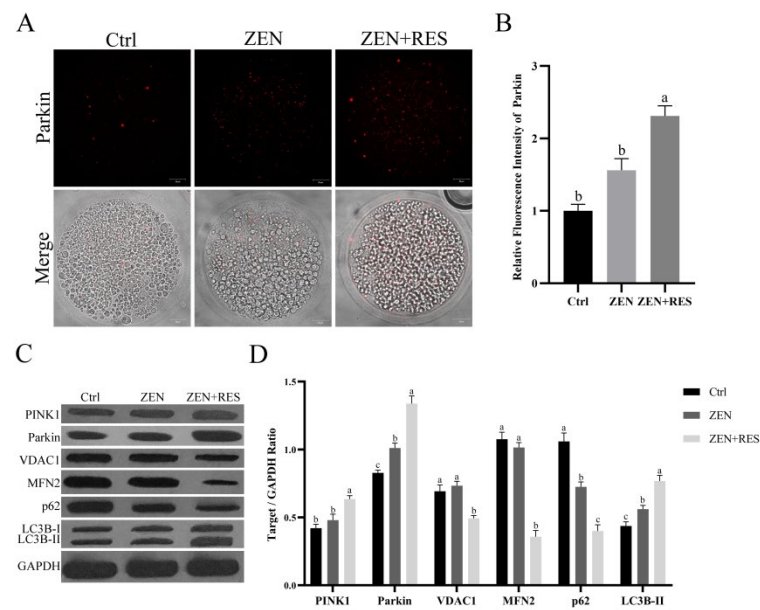


Figure 5. Resveratrol enhanced PINK1/Parkin signaling pathway in zearalenone-exposed porcine oocytes. (A) Fluorescence localization of Parkin. Bar = 20 μ m. Typical intracellular fluorescent distributions were given representing different oocyte treatments. (B) Statistical analysis of relative fluorescence intensity of Parkin. (C) Protein expressions of PINK1/Parkin-mediated mitophagy determined by Western blotting. (D) Statistical analysis of protein expressions. Independent replications were performed three times in each experiment. Different lowercase letters on the statistical graphs indicated significant differences between treatments (p -value < 0.05).

3. Discussion

As a non-steroidal estrogenic mycotoxin, zearalenone is ingested by domestic animals through grains and cereal products and generally causes hypofertility and considerable financial loss in animal husbandry. A previous study on porcine oocytes attributed the toxicity of zearalenone as impairing the function and distribution of organelles, interdicting the extrusion of polar body and disturbing the expansion of cumulus granulosa cells [10]. In vivo research showed that 1.04 mg/kg zearalenone environmental intake induced follicular atresia in pigs, inhibiting proliferation of porcine granulosa cells and inducing its apoptosis and necrosis [23]. However, the dose of zearalenone enriched to porcine follicle fluid was still required to be clarified. On the other side, in vitro dose test on porcine cumulus–oocyte complexes revealed that 10 μ M to 30 μ M zearalenone incubation led to a significant decline in oocyte maturation rate [8] and it further decreased to less than 5% when the concentration of zearalenone up to 50 μ M [24]. A similar study on mouse oocytes also claimed that zearalenone disturbed G2/M transition [25]. In spite of this evidence, however, oxidative-stress-mediated apoptosis was also considered as a plausible mechanism of zearalenone toxicity [9,26], which hinted a potential toxicity effect towards mitochondria and the application of antioxidants. In consideration of these studies, we cultured cumulus–oocyte complexes supplied with 20 μ M zearalenone to explore its effect on the mitochondrial function of porcine oocytes and the potential rescue mechanism. Therefore, in this study, we first investigated the outcome from oocyte meiosis to PA embryo, verifying the fate of oocytes that zearalenone exposure during IVM led to the failure of cleavage and blastosphere formation, whereas the application of resveratrol gained higher embryonic developmental capacity of PA oocytes (Figure 1A–C), which led to further investigations of the antitoxin effects and their mechanism.

In this study, zearalenone was confirmed to disrupt mitochondrial homeostasis, demonstrating structural destruction, depolarization and DNA damage in mitochondria (Figure 2). Dysfunctional mitochondria are less competent to counteract ROS production and the supraphysiological levels of ROS in zearalenone-exposed oocyte led to oxidative

stress (Figure 1D,E). Mitochondria are not only the primary endogenous source of ROS synthesis and release, but also the main target organelle of ROS effects. ROS increases the permeability of the inner-mitochondrial membrane to solutes through activating the mitochondrial permeability transition pore [27], which induces mitochondrial depolarization. Therefore, in this study, zearalenone-induced supraphysiological ROS and structural damage of mitochondria caused a vicious loop between oxidative stress and aggravated mitochondrial dysfunction, in which apoptosis was activated. In addition, zearalenone was previously proved to induce apoptosis and/or autophagy in oocytes [10], spermatogonia [28] and embryo [29], whereas, in this study, we provided evidence that mitophagy was activated in response to zearalenone-induced mitochondrial defects and oxidative stress in porcine oocyte, demonstrated as enhanced mitophagy flux (Figures 3 and 4).

Several studies attempted to mitigate zearalenone-induced impairment and oxidative stress *in vivo* or *in vitro*. *In vivo* research claimed that resveratrol was efficacious in reducing DNA lesions and the modulation of antioxidant enzymes caused by zearalenone intake in rats [30]. *In vitro* comparison in aged mice and humans revealed that about 1.0 μM was a more appropriate concentration of resveratrol than 0.1 μM and 10 μM in IVM medium that induced oocyte maturation and benefitted mitochondrial quality [31]. Meanwhile, another comparison study further revealed that 2 μM was the optimum concentration of resveratrol in a range of 0 to 4 μM to gain increased first polar body extrusion rate and hinder postovulatory aging [21]. A similar study in pigs claimed that reductant Vitamin C prevented hormonal disorders and vulval deformities caused by zearalenone intake [32]. *In vitro* research claimed that melatonin ameliorated oxidative stress, aberrant mitochondria distribution and DNA damage in zearalenone-exposed porcine embryo [29]. In the meantime, we confirmed that resveratrol relieved mitochondrial dysfunction (Figure 2) and prevented oxidative-stress-induced apoptosis (Figure 1) in zearalenone-exposed oocytes through PINK1/Parkin-mediated mitophagy (Figures 3–5).

The progress of apoptosis as well as excessive autophagy generally lead to cell death, while a certain extent of autophagy contributes to maintaining cellular metabolism and environmental homeostasis. In this study, we considered mitophagy as a self-healing mechanism in response of zearalenone infringement towards mitochondria, of which the positive effects of resveratrol-induced autophagy/mitophagy were demonstrated in multiple studies. Resveratrol was verified to enhance SIRT1-mediated autophagy in oocytes against aging [33], alleviating the disorder of mitochondrial biogenesis against benzo(a)pyrene toxicity by promoting mitophagy [34]. A similar effect was also confirmed in flavonoid quercetin, which improved IVM outcomes in porcine by promoting mitophagy, improving mitochondrial function and reducing oxidative stress [35].

Parkin, an E3 ubiquitin ligase belonging to the RING-between-RING family, was involved in the inducement of multiple nerve diseases, including Parkinson's [36], Alzheimer's [37] and Huntington disease [38], of which the pathogenesis was closely related with mitochondrial dysregulation. Moreover, it brought about widespread attention whether the deficiency of Parkin-mediated mitophagy might be a potential pathogenesis of these diseases [39]. Nevertheless, the implementation of PINK1/Parkin-mediated mitophagy was ubiquitin dependent. A noteworthy fact was that MFN1 and MFN2, the ubiquitinated substrates of PINK1/Parkin, were recognized as key regulators of mitochondrial fusion in mammals. Although mitochondria were considered morphologically static organelles, they continuously change their shape in response to a variety of cellular signals, which were known as mitochondrial dynamics [40]. Damaged mitochondria may lose their inner-membrane potential, causing accumulation of toxic ROS, then contaminating other mitochondria through mitochondrial fusion. In this study, the enhanced degradation of MFN2 through the ubiquitin–proteasome proteolytic system was determined when resveratrol co-incubated with zearalenone during IVM, which revealed a synchronization between enhanced clearance through mitophagy and inhibited fusion of damaged mitochondria as the antitoxin effect of resveratrol against zearalenone in porcine oocytes.

This *in vitro* study gave the evidence of phytoalexin resveratrol application showing reproductive toxicity resistance in pigs. However, each oocyte was suspended in follicular fluid of a follicle in ovaries, so the concentration of resveratrol from *in vitro* to *in vivo* needs to consider the absorptivity of RES from blood to follicular fluid and its accumulation effect. The bioavailability of oral RES still needs further *in vivo* studies, since many factors affect its absorption, such as different species, the amount of fat in the diet and drug-delivery methods (oral vs. intraperitoneal injection) et al. [41].

Nevertheless, it occurred with high frequency when livestock underwent a co-exposure between zearalenone and deoxynivalenol. The ecology of deoxynivalenol production often mirrors that of zearalenone, since it is produced by the same fungi and usually detected in crops at the same time. A similar reproductive toxic effect to zearalenone was also detected, of which the exposure of deoxynivalenol towards oocyte hindered the normal progression of meiosis by disrupted meiotic spindle. The inducement of autophagy and apoptosis was also detected in oocytes after deoxynivalenol exposure [42]. Moreover, their co-exposure toward oocytes was confirmed to alter DNA methylation levels [43], which caused the loose embryo developmental capacity [44]. Therefore, whether resveratrol would show a similar resistant effect against deoxynivalenol or their joint toxicity in oocytes through mitophagy remains a worthy research issue.

4. Conclusions

We attributed the oxidative stress and apoptosis of porcine oocytes to functional defects in mitochondria induced by zearalenone during IVM, which further led to embryonic developmental incapacity. Phytoalexin resveratrol alleviated zearalenone-induced mitochondrial dysfunction, oxidative stress and apoptosis by upregulating PINK1/Parkin-mediated mitophagy, which improved embryonic developmental potential. This study proposed a feasible protocol for porcine oocytes to resist reproductive toxicity of estrogenic mycotoxin zearalenone with the application of phytoalexin resveratrol during oocyte maturation.

5. Materials and Methods

5.1. Chemicals

Chemicals applied in this study were purchased from Sigma-Aldrich (St Louis, MO, USA) unless otherwise specified.

5.2. Oocyte Maturation

Prepubertal gilts were slaughtered in a local slaughter house. Their ovaries were subsequently separated from enterocoelia, preserved in 0.9% (*w/v*) saline at 39 °C and transported to laboratory within 1 h. A 10 mL syringe (combining with an 18-gauge needle) was used to aspirate porcine follicular fluid (PFF) from antral follicles, which contained cumulus–oocyte complexes (COCs). After being naturally precipitated for 30 min at 39 °C, the superstratum was centrifuged at 3000 r/min for 15 min and filtered to gain PFF, while the sediment was inspected under microscopy to gain COCs. Every 55 COCs were cultured in a well of four-well dishes, with each well consisting of 500 µL *in vitro* maturation medium [45] and covered with 200 µL mineral oil. 20 µM zearalenone (Pribolab Pte. Ltd., Singapore) with or without 2 µM resveratrol added into maturation medium. The COCs were cultured at 39 °C in a humidified atmosphere of 5% CO₂ for 44 h and transferred into 0.1% hyaluronidase to stripped oocyte from COCs.

5.3. Embryonic Developmental Capacity

PA was performed on cumulus-denuded oocytes after 44 h maturation so as to verify their embryonic developmental capacity. After being washed with PA medium [46] 3 times, cumulus-denuded oocytes were transferred to a microslide 0.5 mm fusion chamber (Model 450, BTX, Holliston, MA, USA) and went through a 1.2 kV/cm direct current pulse in 60 ms by BTX2001 (BTX, Holliston, MA, USA). About 150 electric activated oocytes were cultured in porcine zygote medium-3 [47] at 39 °C in a humidified atmosphere of 5%

CO₂. Number of cleavages was observed and counted at 2 d. Number of blastospheres was counted at 7 d.

5.4. Oocyte ROS Level

Next, 30 oocytes were stained by 50 µM 2',7'-dichlorofluorescein diacetate (DCFH-DA) (S0033, Beyotime, Shanghai, China) for 30 min at 39 °C in a humidified atmosphere of 5% CO₂, then washed 3 times with PBS and inspected by a fluorescence microscope (Olympus, Tokyo City, Japan). Relative fluorescence intensity was analyzed by image J.

5.5. Oocyte Apoptosis

Then, 30 oocytes were stained by 2.5% Annexin V-mCherry (C1069, Beyotime, China) for 30 min at 39 °C in a humidified atmosphere of 5% CO₂, then washed 3 times with PBS and inspected under fluorescence microscope. Oocytes observed with red fluorescence were considered as apoptotic oocytes.

5.6. Intracellular Ultrastructure Observation

The procedures referred to the previous study [46]. In brief, 500 oocytes were fixed in 2.5% glutaraldehyde, embedded in 4% agar, fixed with 1% osmium tetroxide, fully dehydrated with a series of increased concentration of ethanol, replaced with propylene oxide, transferred in Epon-812 and polymerized in polymerization reactor. Ultrathin sections were sliced to form semithin sections, stained with uranyl acetate-lead citrate and observed under transmission electron microscopy.

5.7. Mitochondrial Membrane Potential

Following this, 30 oocytes were stained with 5,5',6,6'-tetrachloro-1,1',3,3'-tetraethylimidocarbocyanine iodide (JC-1) (C2006, Beyotime, China) for 30 min in a humidified atmosphere of 5% CO₂ to determine the $\Delta\Psi_m$. After staining, oocytes were washed with PBS 3 times, inspected under an LSCM and visualized using software ZEN (Carl Zeiss, Germany). When the $\Delta\Psi_m$ was low, JC-1 was kept as monomer which could be detected in green fluorescence, while it formed into aggregation in mitochondria with high $\Delta\Psi_m$ and could be detected as red fluorescence. The ratio of red (JC-1 aggregation) to green (JC-1 monomer) fluorescence intensity represented the $\Delta\Psi_m$.

5.8. Relative mtDNA Copy Number

Next, 100 oocytes were pooled as one sample for total RNA isolation using TaKaRa MiniBEST Universal RNA Extraction Kit (9767, Takara, Kusatsu, Shiga, Japan). PrimeScript RT Master Mix (RR036A, Takara, Japan) and TB Green® Premix Ex Taq™ II (Tli RNaseH Plus, Takara, Japan) were used for reverse transcription and real-time PCR following manufacturers' instruction. ND1, specific primer for coding region of mitochondria DNA, was designed on behalf of mitochondrial DNA copy numbers. Glyceraldehyde-3-phosphate dehydrogenase (GAPDH) was designed as reference gene. The primer sequences were listed as follows. ND1, Forward: TCCTACTGGCCGTAGCATTCT; Reword: TTGAG-GATGTGGCTGGTCGTAG. GAPDH, Forward: CGATGGTGAAGGTCGGAGTG; Reword: TGCCGTGGGTGGAATCATAAC. The results were calculated by $2^{-\Delta\Delta C_t}$ method.

5.9. Immunofluorescence

Oocytes were fixed in 4% paraformaldehyde for 30 min, washed 3 times with 0.1% Tween-20 and transferred to 0.1% Triton X-100 overnight for permeabilization. Permeabilized oocytes were washed 3 times and then blocked with 1% BSA for 1 h.

Blocked oocytes were successively incubated with the primary and secondary antibodies Rabbit anti-Parkin antibody (ab233434, Abcam, Boston, MA, USA) and Goat anti-rabbit IgG H&L (Alexa Fluor® 647) (ab150079, Abcam, USA), washed with PBS 3 times and the fluorescence aggregation of Parkin was observed with LSCM.

For colocalization of LC3B and TOMM20, blocked oocytes were incubated with Rabbit Anti-LC3B (ab192890, Abcam, USA) and Mouse Anti-TOMM20 (ab283317, Abcam, USA) for 1 h, then incubated with secondary antibodies Goat anti-mouse IgG H&L (Alexa Fluor® 488) (ab150113, Abcam, USA) and Goat anti-rabbit IgG H&L (Alexa Fluor® 647) (ab150079, Abcam, USA), washed with PBS 3 times and observed with LSCM. The overlapping coefficient was analyzed using Image J as the fraction of VDAC1 overlapping LC3B.

5.10. Fluorescent Colocalization of Mitophagolysosomes

Then, 30 oocytes were co-stained with Mito-Tracker Green (C1048, Beyotime, China) and Lyso-Tracker Red (C1046, Beyotime, China) following the manufacturer's instructions. Oocytes were then washed 3 times with PBS and observed under LSCM. The colocalization coefficient between the fluorescence of mitochondria and lysosomes was analyzed as the Pearson's coefficient using Image J software, which represented mitophagolysosomes.

5.11. Protein Quantification by Western Blot Assay

For protein extraction, 100 oocytes were gathered and transferred in protein lysis buffer as a sample, with three duplicates for each group and the determination of protein concentration was performed using a BCA Protein Assay Kit (02912E, Cwbiotech, Beijing, China). Western blotting assay was subsequently performed following manufacturers' protocols to ensure the levels of protein expression. The information of primary and secondary antibodies is listed as follows: Rabbit Anti-PINK1 (ab23707, Abcam, USA), Rabbit anti-Parkin (ab233434, Abcam, USA), Rabbit Anti-VDAC1/Porin (ab15895, Abcam, USA), Rabbit anti-Mitofusin 2 (ab124773, Abcam, USA), Rabbit Anti-LC3B, Rabbit Anti-SQSTM1/p62 (ab233207, Abcam, USA), Rabbit Anti-GAPDH (ab9484, Abcam, USA) and the secondary antibody Goat anti-rabbit IgG (H+L) (HRP) (111-035-003, Jackson, West Grove, PA, USA). The expression of GAPDH was determined as a loading control.

5.12. Statistical Analysis

At least three independent replicates were performed in each experiment. Image J was used to determine fluorescence intensity, colocalization coefficient and Western blot quantification. ANOVAs with Duncan multiple comparisons were executed for data comparisons in SPSS Statistics 22 (IBM, Armonk, NY, USA). The results were provided as the mean \pm SEM. Different lowercase letters on the statistical graph indicate significant differences between treatments (p -value < 0.05).

Author Contributions: Conceptualization, D.Z.; Formal analysis, S.Z.; Funding acquisition, D.Z. and J.D.; Investigation, J.X. and L.S.; Methodology, J.D.; Project administration, J.D.; Resources, C.W.; Software, M.H.; Supervision, D.Z.; Validation, J.G.; Visualization, M.H.; Writing—original draft, J.X. and L.S.; Writing—review and editing, J.X. All authors have read and agreed to the published version of the manuscript.

Funding: This research was funded by the National Key Research and Development Plan, grant number 2021YFD1200301; Chongqing Technology Innovation and Application Development Project, grant number CSTC2021-JSCX-DXWTBX0004; and Ningbo Science and Technology Innovation 2025 Major Project, grant number 2019B10023.

Institutional Review Board Statement: The animal study protocol was approved by the Animal Ethics Committee of SHANGHAI ACADEMY OF AGRICULTURAL SCIENCES with the Permit Code: SAASPZ0522057, Approval Date: 1 April 2022. The slaughter and sampling were in accordance with the 'Guidelines on Ethical Treatment of Experimental Animals' (2006) No.398 set by the Ministry of Science and Technology, China.

Informed Consent Statement: Not applicable.

Data Availability Statement: Not applicable.

Acknowledgments: We acknowledge the funding support for this study and the valuable contributions from the MDPI staff.

Conflicts of Interest: The authors declare no conflict of interest.

References

1. Streit, E.; Schwab, C.; Sulyok, M.; Naehrer, K.; Krska, R.; Schatzmayr, G. Multi-mycotoxin screening reveals the occurrence of 139 different secondary metabolites in feed and feed ingredients. *Toxins* **2013**, *5*, 504–523. [[CrossRef](#)]
2. Metzler, M.; Pfeiffer, E.; Hildebrand, A. Zearalenone and its metabolites as endocrine disrupting chemicals. *World Mycotoxin J.* **2010**, *3*, 385–401. [[CrossRef](#)]
3. Gruber-Dorninger, C.; Jenkins, T.; Schatzmayr, G. Global mycotoxin occurrence in feed: A ten-year survey. *Toxins* **2019**, *11*, 375. [[CrossRef](#)]
4. Zinedine, A.; Soriano, J.M.; Molto, J.C.; Manes, J. Review on the toxicity, occurrence, metabolism, detoxification, regulations and intake of zearalenone: An oestrogenic mycotoxin. *Food Chem. Toxicol.* **2007**, *45*, 1–18. [[CrossRef](#)]
5. Xu, Y.; Sun, M.H.; Li, X.H.; Ju, J.Q.; Chen, L.Y.; Sun, Y.R.; Sun, S.C. Modified hydrated sodium calcium aluminosilicate-supplemented diet protects porcine oocyte quality from zearalenone toxicity. *Environ. Mol. Mutagenesis* **2021**, *62*, 124–132. [[CrossRef](#)]
6. EFSA, K.H.; Alexander, J. Risks for animal health related to the presence of zearalenone and its modified forms in feed. *J. EFSA J.* **2017**, *15*, e04851.
7. Liu, J.; Applegate, T. Zearalenone (ZEN) in livestock and poultry: Dose, toxicokinetics, toxicity and estrogenicity. *Toxins* **2020**, *12*, 377. [[CrossRef](#)]
8. Han, J.; Wang, T.; Fu, L.; Shi, L.-Y.; Zhu, C.-C.; Liu, J.; Zhang, Y.; Cui, X.-S.; Kim, N.-H.; Sun, S.-C. Altered oxidative stress, apoptosis/autophagy, and epigenetic modifications in Zearalenone-treated porcine oocytes. *Toxicol. Res.* **2015**, *4*, 1184–1194. [[CrossRef](#)]
9. Yao, X.; Jiang, H.; Gao, Q.; Li, Y.-H.; Xu, Y.N.; Kim, N.-H. Melatonin alleviates defects induced by zearalenone during porcine embryo development. *Theriogenology* **2020**, *151*, 66–73. [[CrossRef](#)]
10. Wang, Y.; Xing, C.-H.; Chen, S.; Sun, S.-C. Zearalenone exposure impairs organelle function during porcine oocyte meiotic maturation. *Theriogenology* **2022**, *177*, 22–28. [[CrossRef](#)]
11. Wang, J.; Li, M.; Zhang, W.; Gu, A.; Dong, J.; Li, J.; Shan, A. Protective effect of n-acetylcysteine against oxidative stress induced by zearalenone via mitochondrial apoptosis pathway in SIEC02 cells. *Toxins* **2018**, *10*, 407. [[CrossRef](#)]
12. Boyman, L.; Karbowski, M.; Lederer, W.J. Regulation of mitochondrial ATP production: Ca²⁺ signaling and quality control. *Trends Mol. Med.* **2020**, *26*, 21–39. [[CrossRef](#)]
13. Shen, Q.; Liu, Y.; Li, H.; Zhang, L. Effect of mitophagy in oocytes and granulosa cells on oocyte quality. *Biol. Reprod.* **2021**, *104*, 294–304. [[CrossRef](#)]
14. Levine, B.; Kroemer, G. Biological functions of autophagy genes: A disease perspective. *Cell* **2019**, *176*, 11–42. [[CrossRef](#)]
15. Geisler, S.; Holmström, K.M.; Skujat, D.; Fiesel, F.C.; Rothfuss, O.C.; Kahle, P.J.; Springer, W. PINK1/Parkin-mediated mitophagy is dependent on VDAC1 and p62/SQSTM1. *Nat. Cell Biol.* **2010**, *12*, 119–131. [[CrossRef](#)]
16. Chan, N.C.; Salazar, A.M.; Pham, A.H.; Sweredoski, M.J.; Kolawa, N.J.; Graham, R.L.; Hess, S.; Chan, D.C. Broad activation of the ubiquitin–proteasome system by Parkin is critical for mitophagy. *Hum. Mol. Genet.* **2011**, *20*, 1726–1737. [[CrossRef](#)]
17. Narendra, D.; Walker, J.E.; Youle, R. Mitochondrial quality control mediated by PINK1 and Parkin: Links to parkinsonism. *Cold Spring Harb. Perspect. Biol.* **2012**, *4*, a011338. [[CrossRef](#)]
18. Exner, N.; Lutz, A.K.; Haass, C.; Winklhofer, K.F. Mitochondrial dysfunction in Parkinson’s disease: Molecular mechanisms and pathophysiological consequences. *EMBO J.* **2012**, *31*, 3038–3062. [[CrossRef](#)]
19. De Vos, M.; Grynberg, M.; Ho, T.M.; Yuan, Y.; Albertini, D.F.; Gilchrist, R.B. Perspectives on the development and future of oocyte IVM in clinical practice. *J. Assist. Reprod. Genet.* **2021**, *38*, 1265–1280. [[CrossRef](#)]
20. Hara, T.; Kin, A.; Aoki, S.; Nakamura, S.; Shirasuna, K.; Kuwayama, T.; Iwata, H. Resveratrol enhances the clearance of mitochondrial damage by vitrification and improves the development of vitrified-warmed bovine embryos. *PLoS ONE* **2018**, *13*, e0204571. [[CrossRef](#)]
21. Abbasi, B.; Dong, Y.; Rui, R. Resveratrol hinders postovulatory aging by modulating oxidative stress in porcine oocytes. *Molecules* **2021**, *26*, 6346. [[CrossRef](#)]
22. Zhou, J.; Xue, Z.; He, H.-N.; Liu, X.; Yin, S.-Y.; Wu, D.-Y.; Zhang, X.; Schatten, H.; Miao, Y.-L. Resveratrol delays postovulatory aging of mouse oocytes through activating mitophagy. *Aging* **2019**, *11*, 11504. [[CrossRef](#)]
23. Dai, M.; Jiang, S.; Yuan, X.; Yang, W.; Yang, Z.; Huang, L. Effects of zearalenone-diet on expression of ghrelin and PCNA genes in ovaries of post-weaning piglets. *Anim. Reprod. Sci.* **2016**, *168*, 126–137. [[CrossRef](#)]
24. Lu, Y.; Zhang, Y.; Liu, J.-Q.; Zou, P.; Jia, L.; Su, Y.-T.; Sun, Y.-R.; Sun, S.-C. Comparison of the toxic effects of different mycotoxins on porcine and mouse oocyte meiosis. *PeerJ* **2018**, *6*, e5111. [[CrossRef](#)]
25. Ji, Y.-M.; Zhang, K.-H.; Pan, Z.-N.; Ju, J.-Q.; Zhang, H.-L.; Liu, J.-C.; Wang, Y.; Sun, S.-C. High-dose zearalenone exposure disturbs G2/M transition during mouse oocyte maturation. *Reprod. Toxicol.* **2022**, *110*, 172–179. [[CrossRef](#)]
26. Feng, Y.-Q.; Zhao, A.-H.; Wang, J.-J.; Tian, Y.; Yan, Z.-H.; Dri, M.; Shen, W.; De Felici, M.; Li, L. Oxidative stress as a plausible mechanism for zearalenone to induce genome toxicity. *Gene* **2022**, *829*, 146511. [[CrossRef](#)]
27. Wang, Z.-H.; Clark, C.; Geisbrecht, E.R. Drosophila clueless is involved in Parkin-dependent mitophagy by promoting VCP-mediated Marf degradation. *Hum. Mol. Genet.* **2016**, *25*, 1946–1964. [[CrossRef](#)]

28. Lee, R.; Kim, D.-W.; Lee, W.-Y.; Park, H.-J. Zearalenone Induces Apoptosis and Autophagy in a Spermatogonia Cell Line. *Toxins* **2022**, *14*, 148. [[CrossRef](#)]
29. Xu, Y.; Zhang, K.-H.; Sun, M.-H.; Lan, M.; Wan, X.; Zhang, Y.; Sun, S.-C. Protective effects of melatonin against zearalenone toxicity on porcine embryos in vitro. *Front. Pharmacol.* **2019**, *10*, 327. [[CrossRef](#)]
30. Virk, P.; Al-Mukhaizeem, N.A.R.; Morebah, S.H.B.; Fouad, D.; Elobeid, M. Protective effect of resveratrol against toxicity induced by the mycotoxin, zearalenone in a rat model. *Food Chem. Toxicol.* **2020**, *146*, 111840. [[CrossRef](#)]
31. Liu, M.-J.; Sun, A.-G.; Zhao, S.-G.; Liu, H.; Ma, S.-Y.; Li, M.; Huai, Y.-X.; Zhao, H.; Liu, H.-B. Resveratrol improves in vitro maturation of oocytes in aged mice and humans. *Fertil. Steril.* **2018**, *109*, 900–907. [[CrossRef](#)]
32. Su, Y.; Sun, Y.; Ju, D.; Chang, S.; Shi, B.; Shan, A. The detoxification effect of vitamin C on zearalenone toxicity in piglets. *Ecotoxicol. Environ. Saf.* **2018**, *158*, 284–292. [[CrossRef](#)] [[PubMed](#)]
33. Sugiyama, M.; Kawahara-Miki, R.; Kawana, H.; Shirasuna, K.; Kuwayama, T.; Iwata, H. Resveratrol-induced mitochondrial synthesis and autophagy in oocytes derived from early antral follicles of aged cows. *J. Reprod. Dev.* **2015**, *61*, 251–259. [[CrossRef](#)]
34. Chen, K.-G.; Kang, R.-R.; Sun, Q.; Liu, C.; Ma, Z.; Liu, K.; Deng, Y.; Liu, W.; Xu, B. Resveratrol ameliorates disorders of mitochondrial biogenesis and mitophagy in rats continuously exposed to benzo (a) pyrene from embryonic development through adolescence. *Toxicology* **2020**, *442*, 152532. [[CrossRef](#)]
35. Cao, Y.; Zhao, H.; Wang, Z.; Zhang, C.; Bian, Y.; Liu, X.; Zhang, C.; Zhang, X.; Zhao, Y. Quercetin promotes in vitro maturation of oocytes from humans and aged mice. *Cell Death Dis.* **2020**, *11*, 1–15. [[CrossRef](#)]
36. Imai, Y. PINK1-Parkin signaling in Parkinson's disease: Lessons from *Drosophila*. *Neurosci. Res.* **2020**, *159*, 40–46. [[CrossRef](#)]
37. Quinn, P.M.; Moreira, P.L.; Ambrósio, A.F.; Alves, C.H. PINK1/PARKIN signalling in neurodegeneration and neuroinflammation. *Acta Neuropathol. Commun.* **2020**, *8*, 1–20. [[CrossRef](#)]
38. Aladdin, A.; Király, R.; Boto, P.; Regdon, Z.; Tar, K. Juvenile Huntington's Disease Skin Fibroblasts Respond with Elevated Parkin Level and Increased Proteasome Activity as a Potential Mechanism to Counterbalance the Pathological Consequences of Mutant Huntingtin Protein. *Int. J. Mol. Sci.* **2019**, *20*, 5338. [[CrossRef](#)]
39. Roverato, N.D.; Sailer, C.; Catone, N.; Aichem, A.; Stengel, F.; Groettrup, M. Parkin is an E3 ligase for the ubiquitin-like modifier FAT10, which inhibits Parkin activation and mitophagy. *Cell Rep.* **2021**, *34*, 108857. [[CrossRef](#)]
40. Zungu, M.; Schisler, J.; Willis, M.S. All the little pieces. –Regulation of mitochondrial fusion and fission by ubiquitin and small ubiquitin-like modifier and their potential relevance in the heart.–. *Circ. J.* **2011**, *75*, 2513–2521. [[CrossRef](#)]
41. Smoliga, J.M.; Blanchard, O. Enhancing the delivery of resveratrol in humans: If low bioavailability is the problem, what is the solution? *Molecules* **2014**, *19*, 17154–17172. [[CrossRef](#)] [[PubMed](#)]
42. Han, J.; Wang, Q.-C.; Zhu, C.-C.; Liu, J.; Zhang, Y.; Cui, X.-S.; Kim, N.-H.; Sun, S.-C. Deoxynivalenol exposure induces autophagy/apoptosis and epigenetic modification changes during porcine oocyte maturation. *Toxicol. Appl. Pharmacol.* **2016**, *300*, 70–76. [[CrossRef](#)] [[PubMed](#)]
43. Zhu, C.-C.; Hou, Y.-J.; Han, J.; Liu, H.-L.; Cui, X.-S.; Kim, N.-H.; Sun, S.-C. Effect of mycotoxin-containing diets on epigenetic modifications of mouse oocytes by fluorescence microscopy analysis. *Microsc. Microanal.* **2014**, *20*, 1158–1166. [[CrossRef](#)] [[PubMed](#)]
44. Malekinejad, H.; Schoevers, E.J.; Daemen, I.J.; Zijlstra, C.; Colenbrander, B.; Fink-Gremmels, J.; Roelen, B.A. Exposure of oocytes to the Fusarium toxins zearalenone and deoxynivalenol causes aneuploidy and abnormal embryo development in pigs. *Biol. Reprod.* **2007**, *77*, 840–847. [[CrossRef](#)]
45. Xu, J.; Zhang, D.; Ju, S.; Sun, L.; Zhang, S.; Wu, C.; Rui, R.; Dai, J. Mitophagy is involved in the mitochondrial dysfunction of vitrified porcine oocytes. *Mol. Reprod. Dev.* **2021**, *88*, 427–436. [[CrossRef](#)]
46. Xu, J.; Sun, L.; Wu, C.; Zhang, S.; Ju, S.; Rui, R.; Zhang, D.; Dai, J. Involvement of PINK1/Parkin-mediated mitophagy in mitochondrial functional disruption under oxidative stress in vitrified porcine oocytes. *Theriogenology* **2021**, *174*, 160–168. [[CrossRef](#)]
47. Yoshioka, K.; Suzuki, C.; Tanaka, A.; Anas, I.M.-K.; Iwamura, S. Birth of piglets derived from porcine zygotes cultured in a chemically defined medium. *Biol. Reprod.* **2002**, *66*, 112–119. [[CrossRef](#)]